

# Selective naked-eye cyanide detection in aqueous media using a carbazole-derived fluorescent dye

Rajendra Kumar Konidena and K. R. Justin Thomas\*

*Organic Materials Laboratory, Department of Chemistry, Indian Institute of Technology Roorkee,  
Roorkee – 247 667, India.*

\*Corresponding author. E-mail: krjt8fcy@iitr.ac.in; Phone: +91-1332-285376.

## Electronic Supplementary Information

<b>Fig. S1</b>	Absorption spectra of <b>3b</b> in the presence of different anions	S2
<b>Fig. S2</b>	Absorption changes for <b>3b</b> on addition of cyanide in aqueous acetonitrile	S2
<b>Fig. S3</b>	Time dependent absorption changes of <b>3a</b> (left) and <b>3b</b> (right) upon addition of cyanide anion	S3
<b>Fig. S4</b>	Kinetics of sensor <b>3b</b> action	S3
<b>Fig. S5</b>	Jobs plot for <b>3b</b>	S4
	Detection limit determination	S5
<b>Fig. S6</b>	$^1\text{H}$ NMR spectral changes observed for the dye <b>3b</b> on addition of various amounts of cyanide in DMSO-d <sub>6</sub>	S6
<b>Fig. S7</b>	Optimized geometries for <b>3a</b> , <b>3b</b> , <b>3a-CN</b> , and <b>3b-CN</b>	S7
<b>Fig. S8</b>	Absorbance response of <b>3b</b> in the presence of 30 eq. other anions and 2 equiv of CN <sup>-</sup>	S5
	Detection limit determination	S7
<b>Fig. S9</b>	Ratiometric absorbance changes ( $\text{A}_{330}/\text{A}_{405}$ ) of <b>3b</b> on addition of 2 equiv of CN <sup>-</sup> and 10 equiv of other anions. Black bars indicate the blank and various anions, and red bars indicate the addition of CN <sup>-</sup> to the interfering anions	S8
<b>Table S1</b>	Computed vertical transition energies and their oscillator strengths and configurations for the dyes	S9
<b>Fig. S10</b>	$^1\text{H}$ NMR spectra for <b>2a</b> in CDCl <sub>3</sub>	S10
<b>Fig. S11</b>	$^{13}\text{C}$ NMR spectra for <b>2a</b> in CDCl <sub>3</sub>	S10
<b>Fig. S12</b>	$^1\text{H}$ NMR spectra for <b>2b</b> in CDCl <sub>3</sub>	S11
<b>Fig. S13</b>	$^{13}\text{C}$ NMR spectra for <b>2b</b> in CDCl <sub>3</sub>	S11
<b>Fig. S14</b>	$^1\text{H}$ NMR spectra for <b>3a</b> in CDCl <sub>3</sub>	S12
<b>Fig. S15</b>	$^{13}\text{C}$ NMR spectra for <b>3a</b> in CDCl <sub>3</sub>	S12
<b>Fig. S16</b>	$^1\text{H}$ NMR spectra for <b>3b</b> in CDCl <sub>3</sub>	S13
<b>Fig. S17</b>	$^{13}\text{C}$ NMR spectra for <b>3b</b> in CDCl <sub>3</sub>	S13

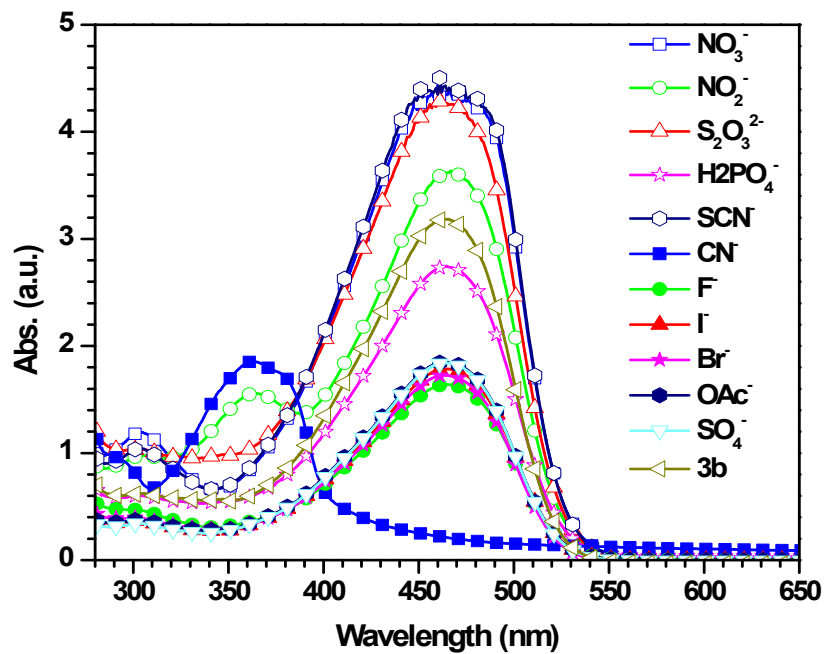


**Fig. S1** Absorption spectra of **3b** in the presence of different anions.

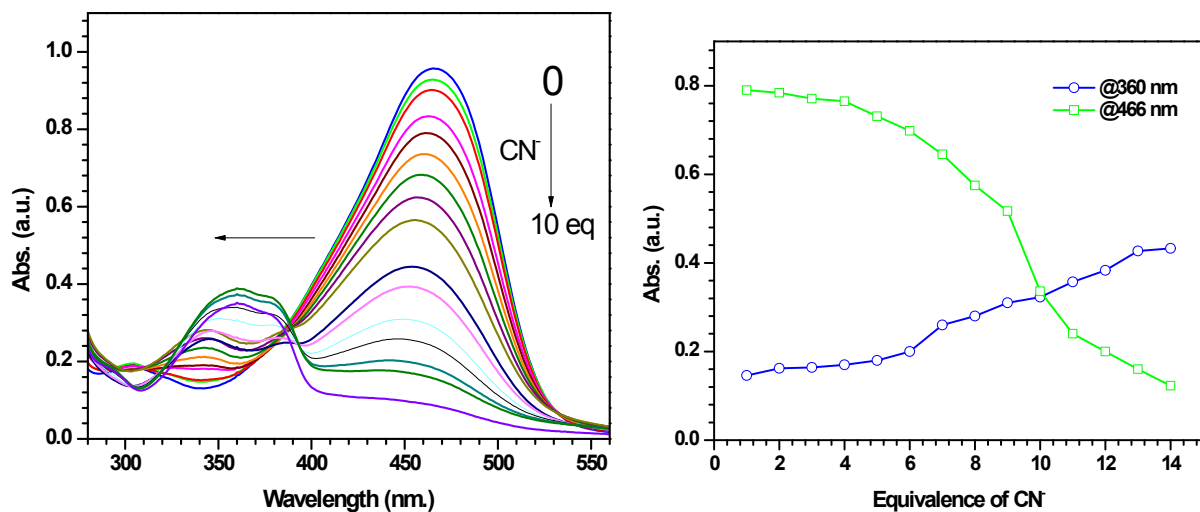


**Fig. S2** Absorption changes for **3b** on addition of cyanide in aqueous acetonitrile.

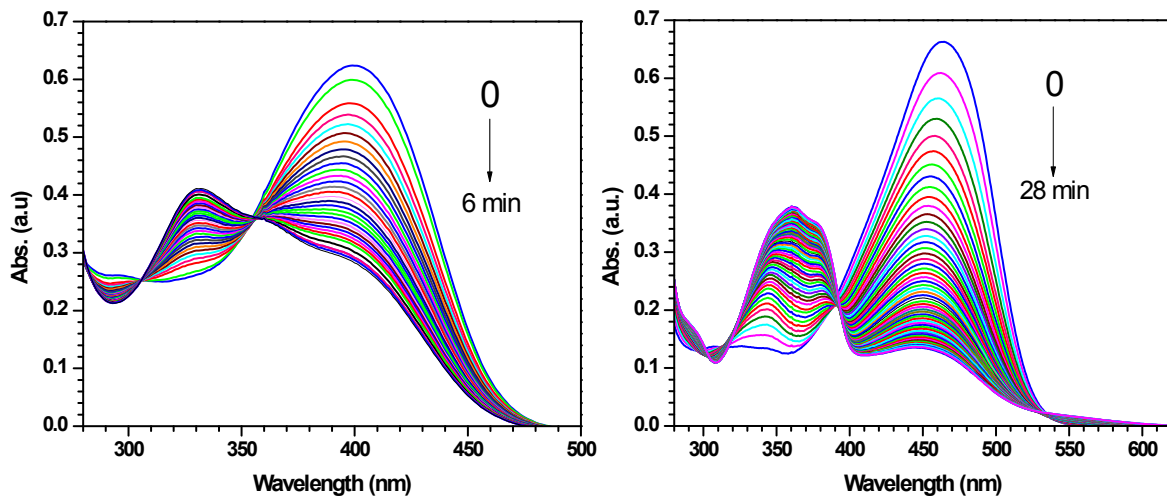


**Fig. S3** Time dependent absorption changes of **3a** (left) and **3b** (right) upon addition of 2 equiv. and 10 equiv. of  $\text{CN}^-$  respectively.

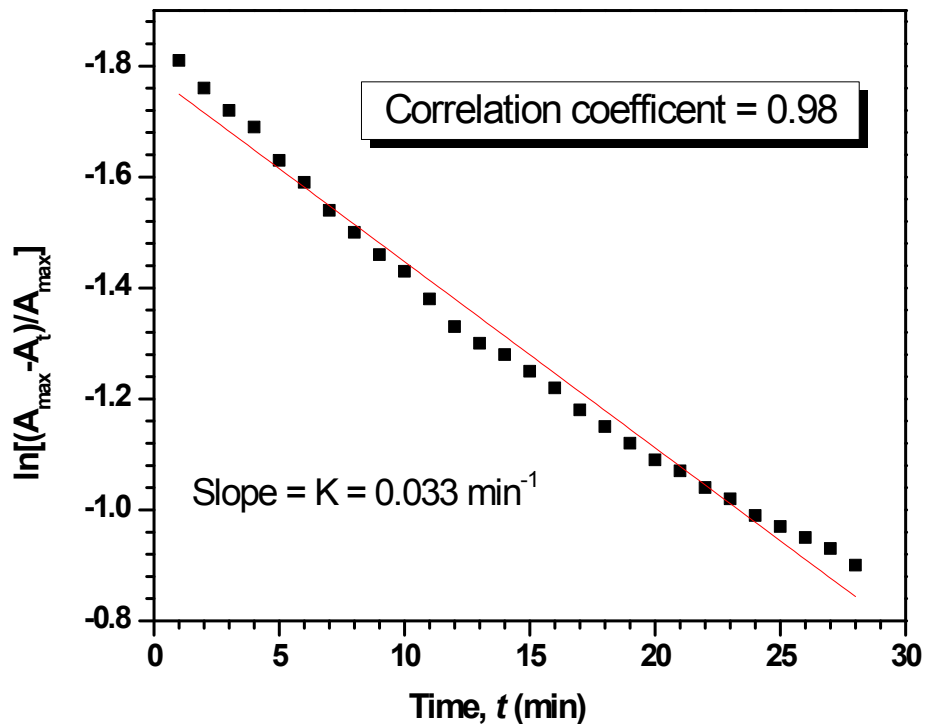


**Fig. S4** Kinetics of sensor **3b** action.

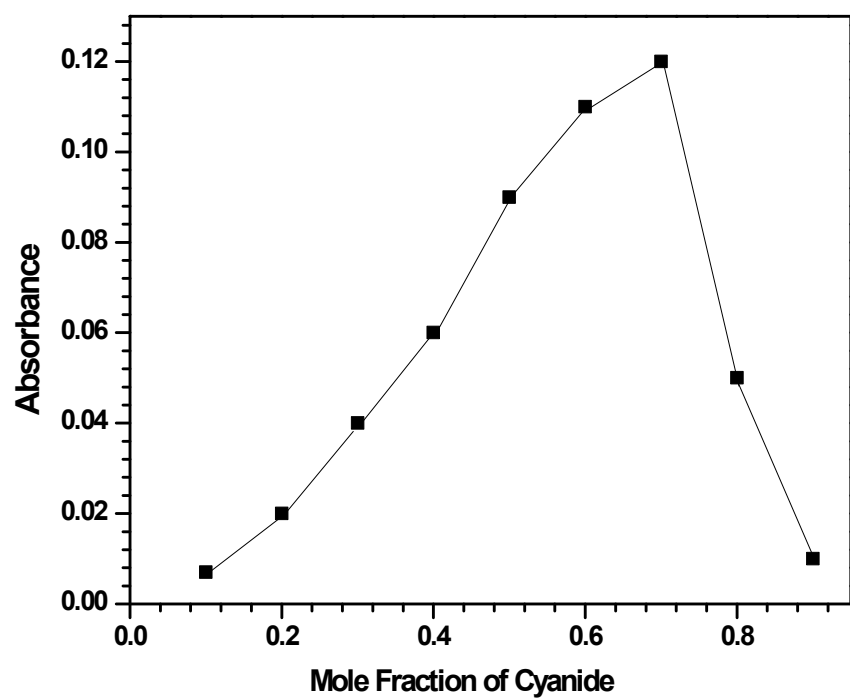


**Fig. S5** Jobs plot for **3b**.

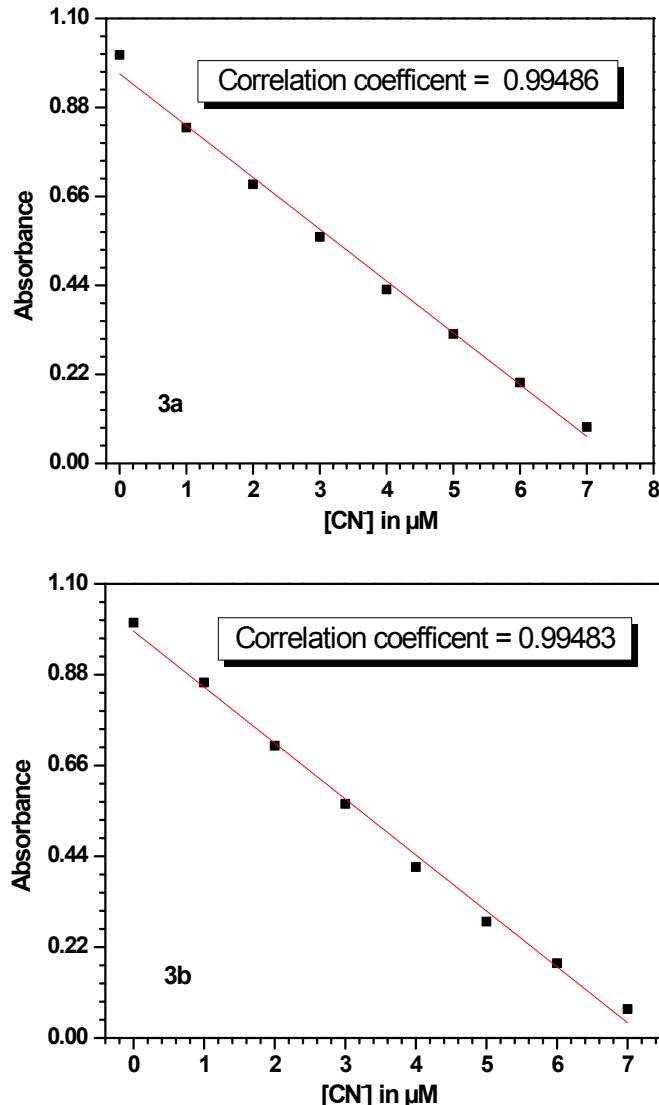
## Detection limit determination

The detection limit of the probes **3a** and **3b** for cyanide was estimated by using the formula,

$$Detection\ limit = \frac{k \times \sigma}{S}$$

Where  $k = 3$ ,  $\sigma$  is the standard deviation of the blank solution and  $S$  is the slope of the calibration curve.

The calibration graphs observed for the dyes **3a** and **3b** are shown below:



Dye	$\sigma$	$S, \mu\text{M}^{-1}$	Detection limit, $\mu\text{M}$
<b>3a</b>	0.0054	0.128	0.136
<b>3b</b>	0.0063	0.135	0.140

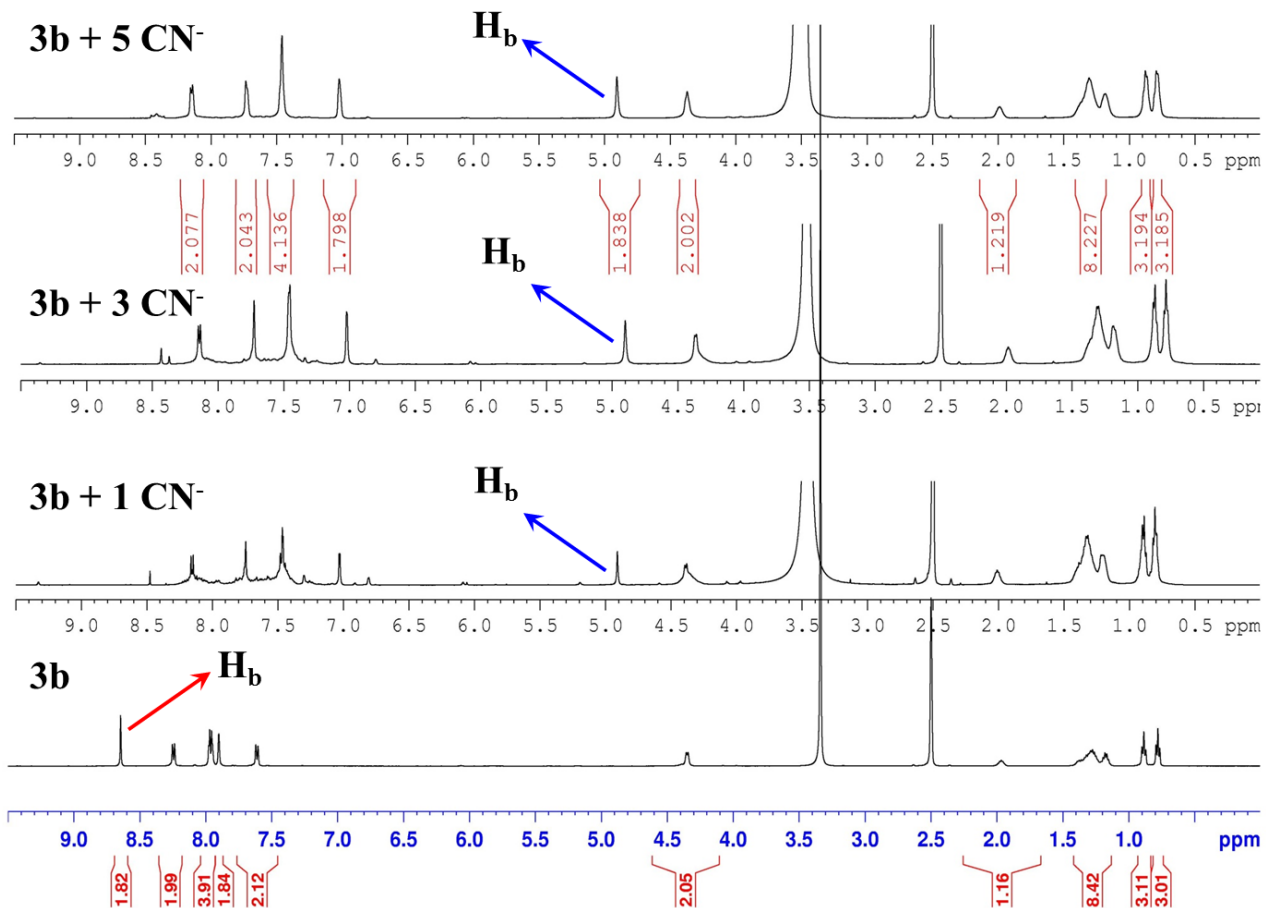
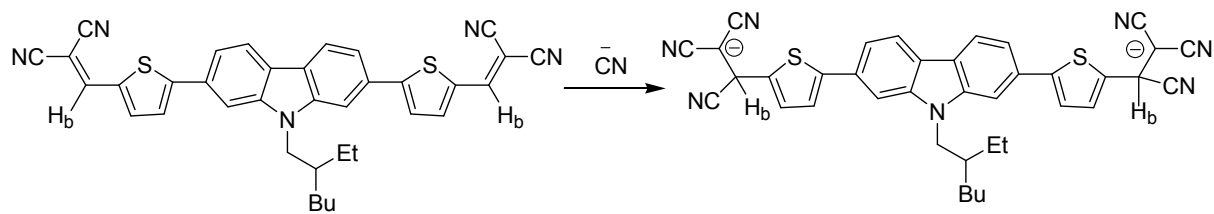


**Fig. S6** <sup>1</sup>H NMR spectral changes observed for the dye **3b** on addition of various amounts of cyanide in DMSO-d<sub>6</sub>.

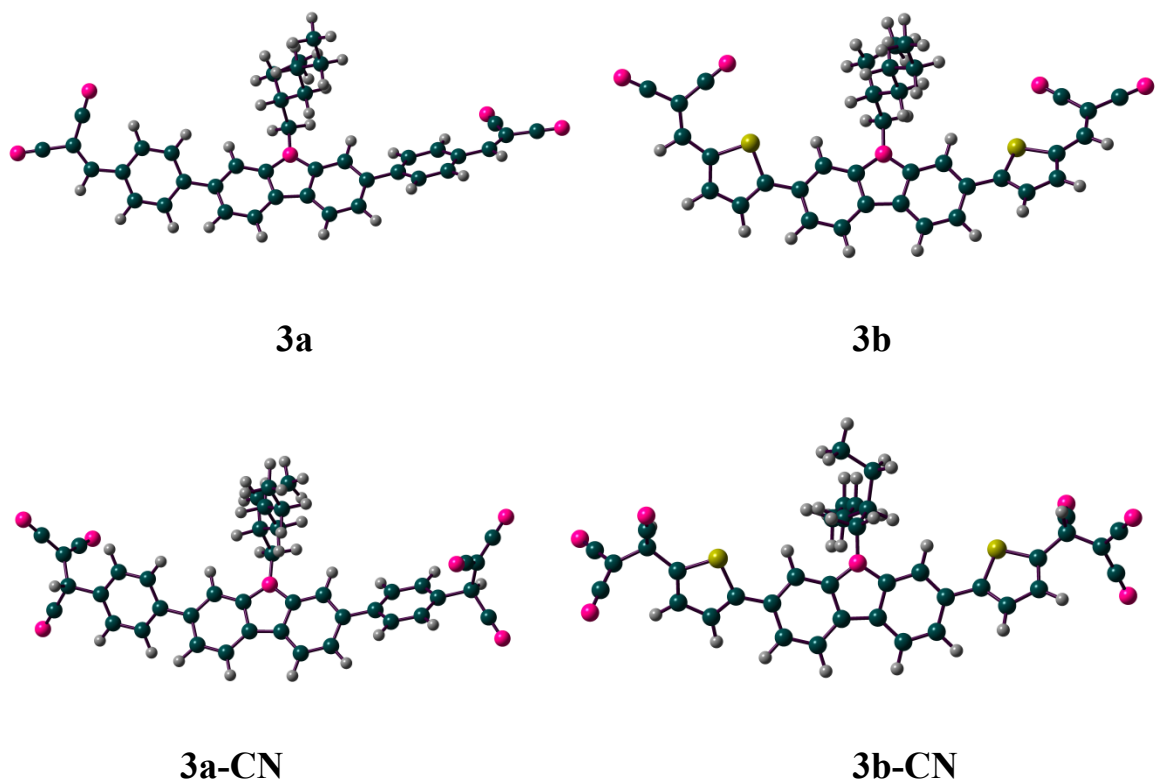


**Fig. S7** Optimized geometries for **3a**, **3b**, **3a-CN<sup>-</sup>**, and **3b-CN<sup>-</sup>**.

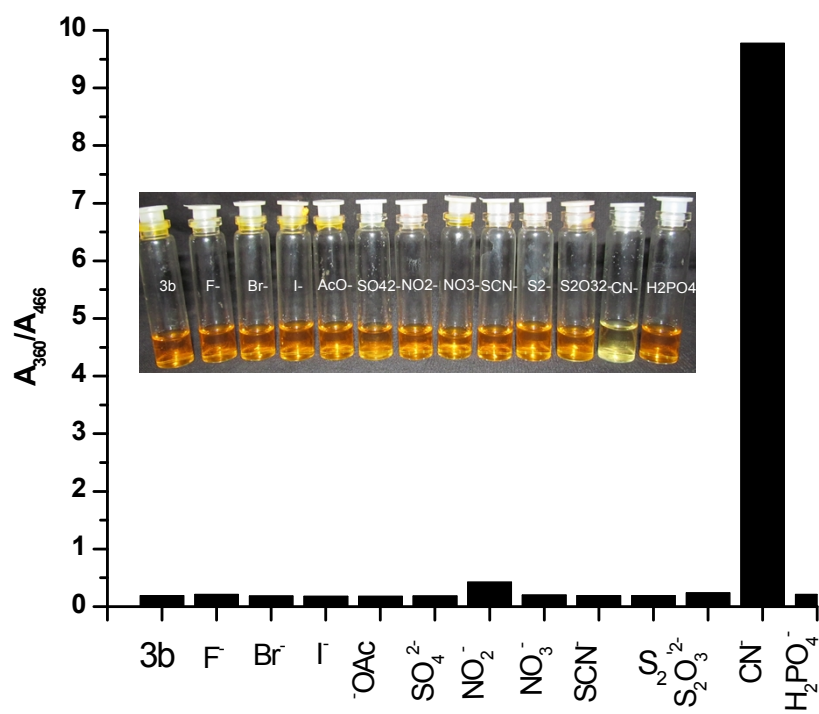


**Fig. S8** Absorbance response of **3b** upon addition of 10 equiv of other anions and 2 eq of CN<sup>-</sup>.

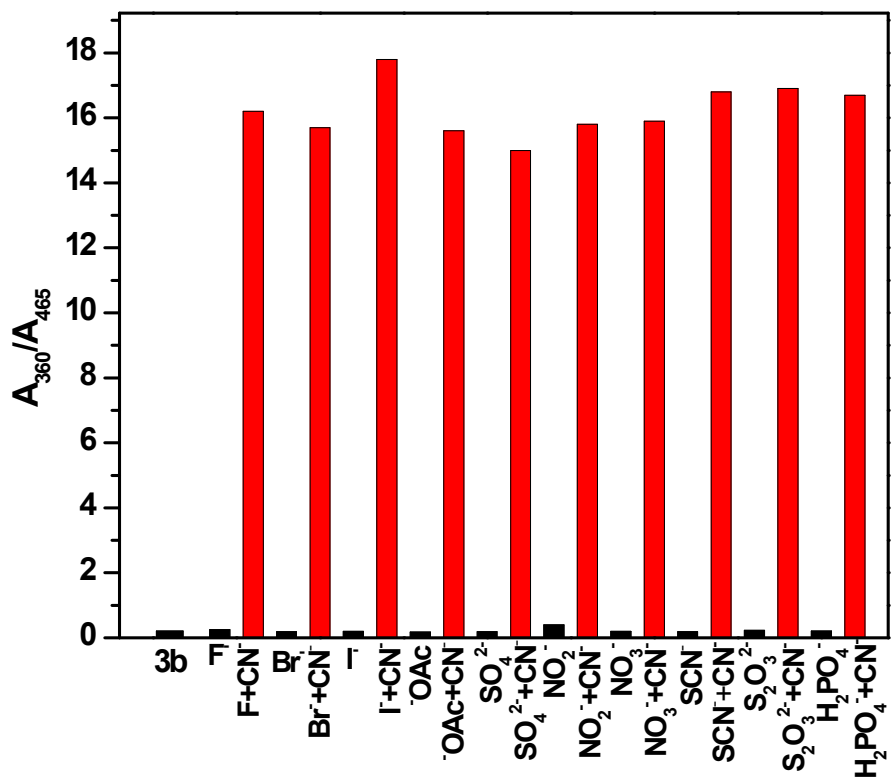


**Fig. S9** Ratiometric absorbance changes ( $A_{330}/A_{405}$ ) of **3b** on addition of 2 equiv of  $\text{CN}^-$  and 10 equiv of other anions. Black bars indicate the blank and various anions, and red bars indicate the addition of  $\text{CN}^-$  to the interfering anions.

**Table S1** Computed vertical transition energies and their oscillator strengths and configurations for the dyes.

Dye	$\lambda_{\text{max}}$ , nm	f	configuration
<b>3a</b>	457.7	1.3582	HOMO-1 → LUMO (96%)
	338.5	0.1077	HOMO-2 → LUMO (98%)
	331.5	0.6820	HOMO-2 → LUMO+1 (93%)
	310.3	0.4822	HOMO-3 → LUMO (63%), HOMO-1 → LUMO+2 (28%)
<b>3b</b>	492.1	1.3592	HOMO → LUMO (99%)
	377.5	0.3741	HOMO-2 → LUMO (89%), HOMO → LUMO+1 (11%)
	361.7	0.3144	HOMO-2 → LUMO+1 (92%)
	329.6	0.1159	HOMO-3 → LUMO (66%), HOMO → LUMO+2 (32%)
<b>3a-CN</b>	330.7	1.2431	HOMO-1 → LUMO
<b>3b-CN</b>	373.6	1.4307	HOMO-2 → LUMO

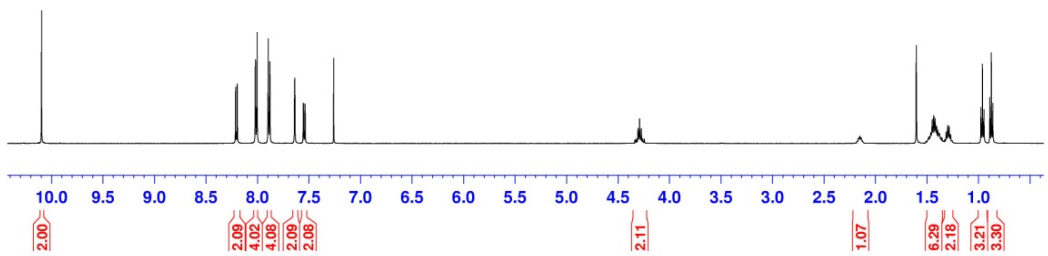
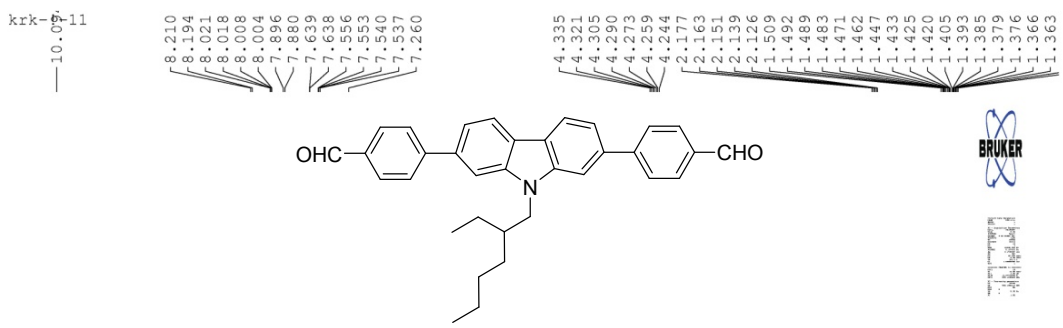


**Fig. S10**  $^1\text{H}$  NMR spectra for **2a** in  $\text{CDCl}_3$ .

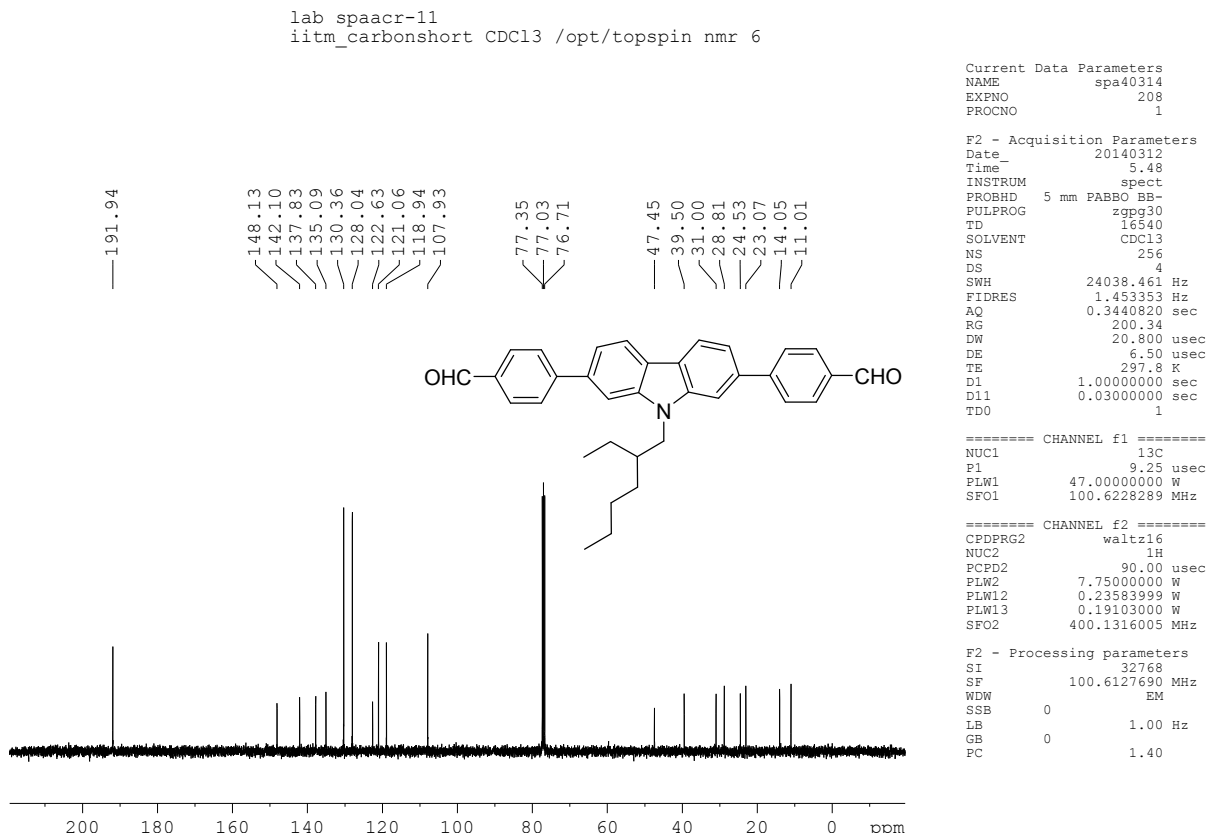


**Fig. S11**  $^{13}\text{C}$ -NMR spectra of compound **2a**.

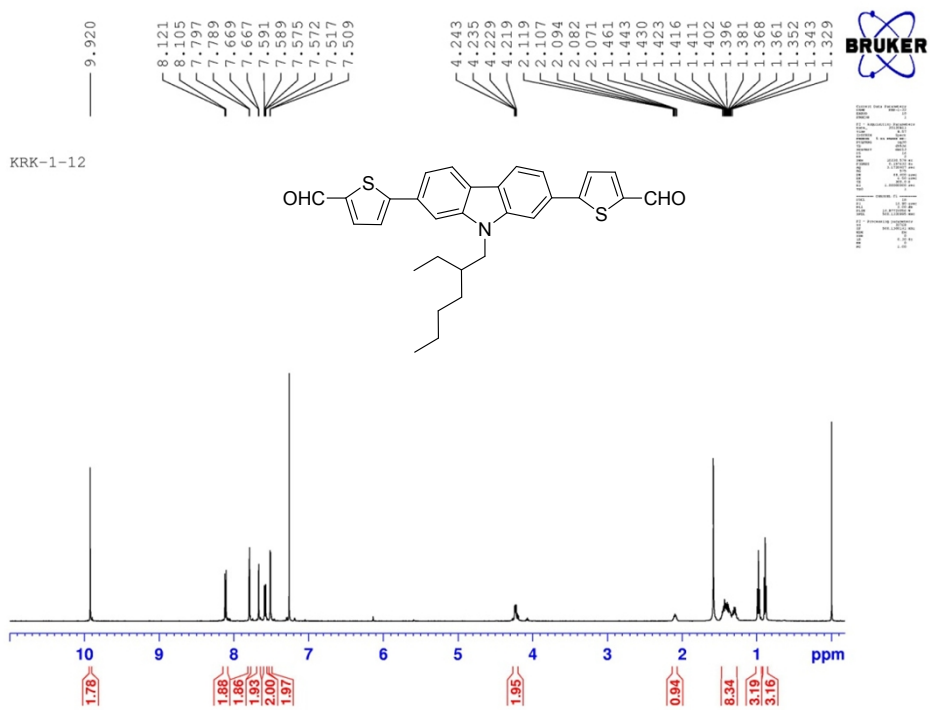


**Fig. S12**  $^1\text{H}$  NMR spectra for **2b** in  $\text{CDCl}_3$ .

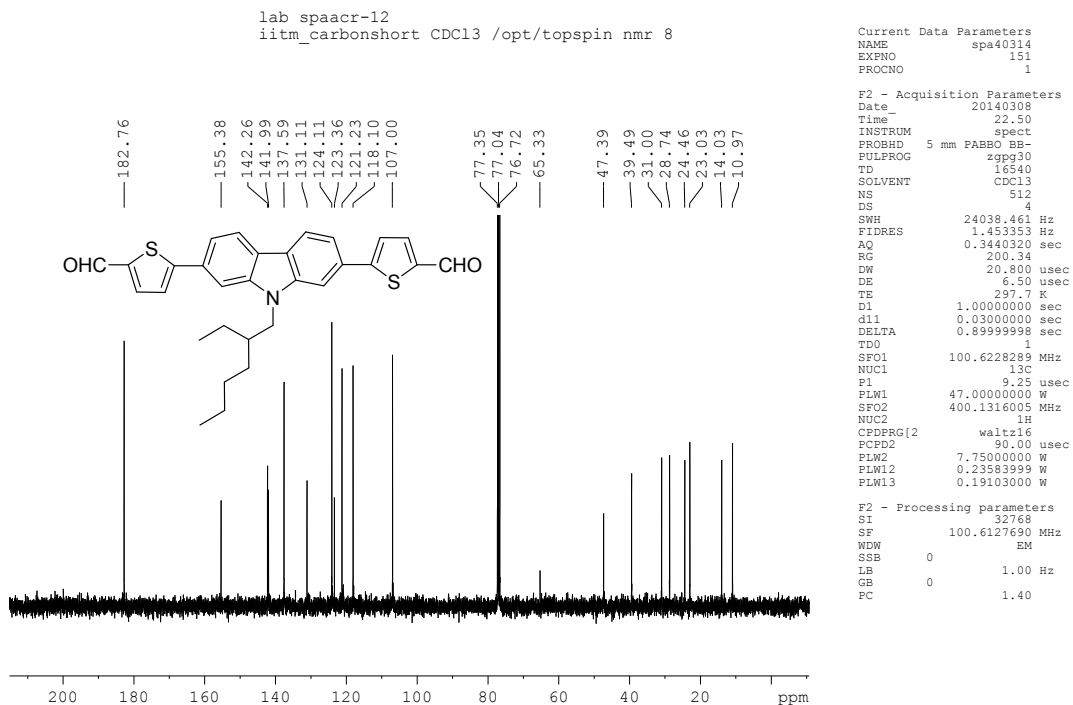


**Fig. S13**  $^{13}\text{C}$  NMR spectra for **2b** in  $\text{CDCl}_3$ .

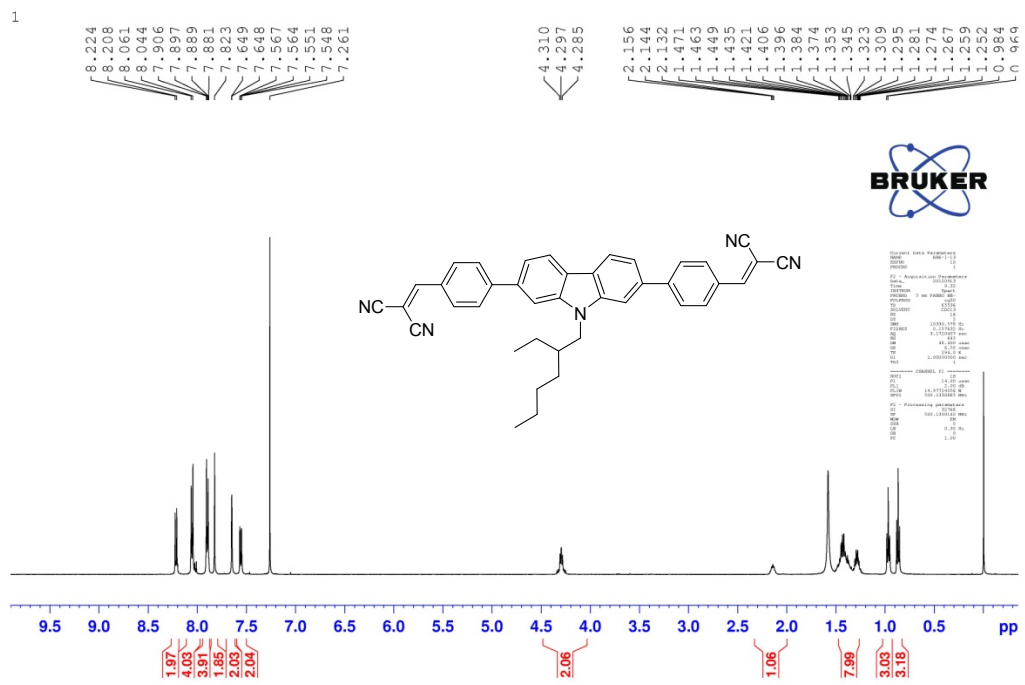
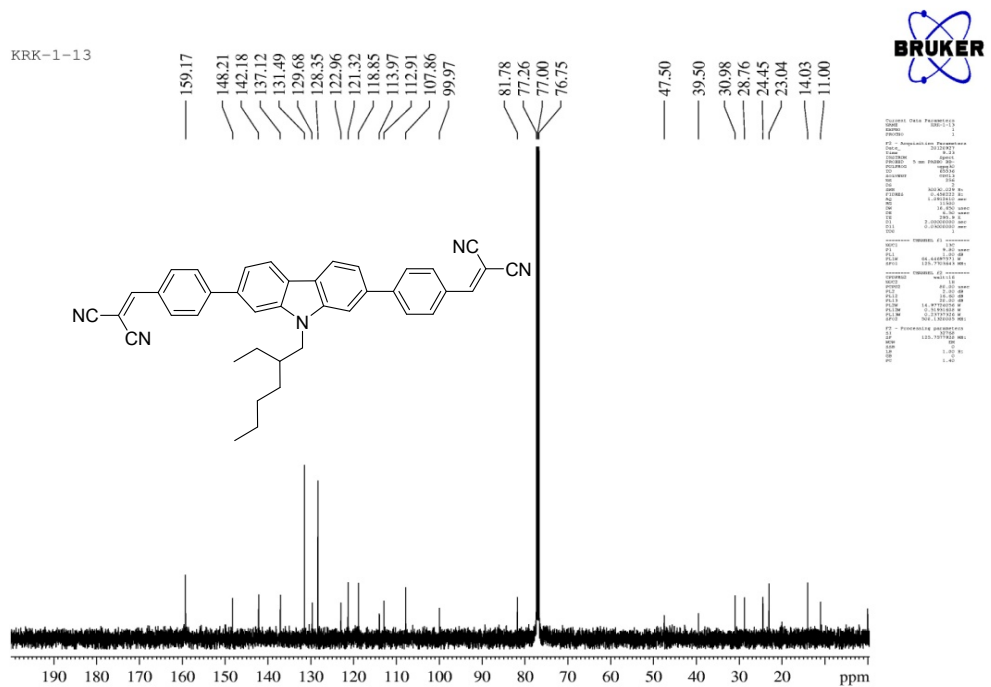


**Fig. S14**  $^1\text{H}$  NMR spectra for **3a** in  $\text{CDCl}_3$ .



**S15**  $^{13}\text{C}$  NMR spectra for **3a**  $\text{CDCl}_3$ .

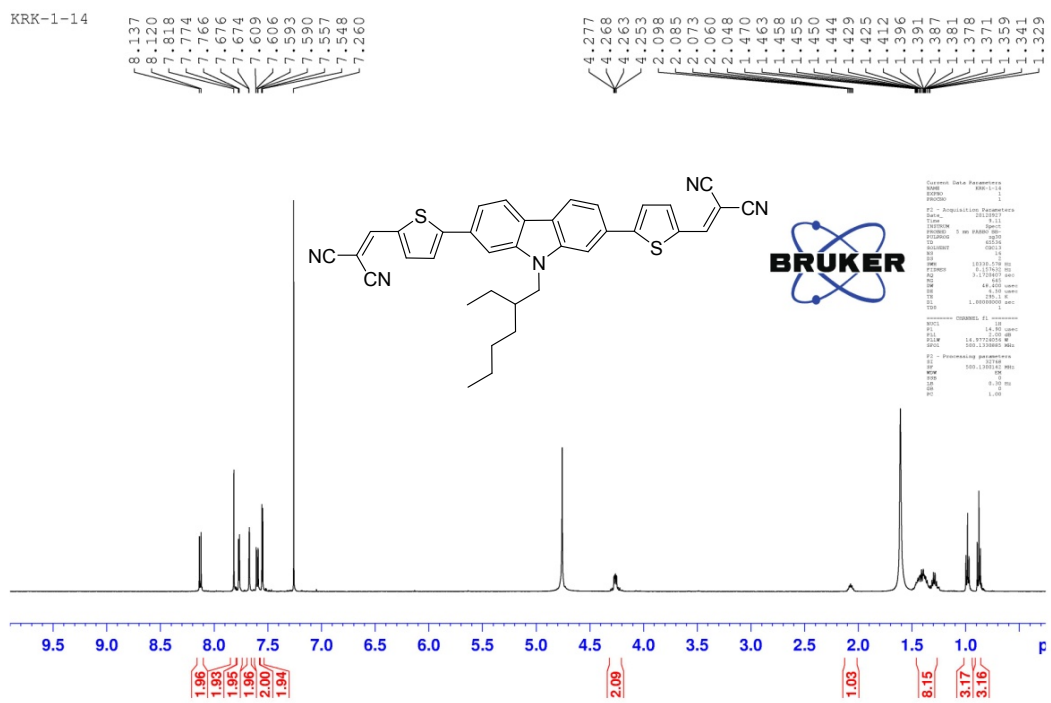


**Fig. S16**  $^1\text{H}$  NMR spectra for **3b** in  $\text{CDCl}_3$ .

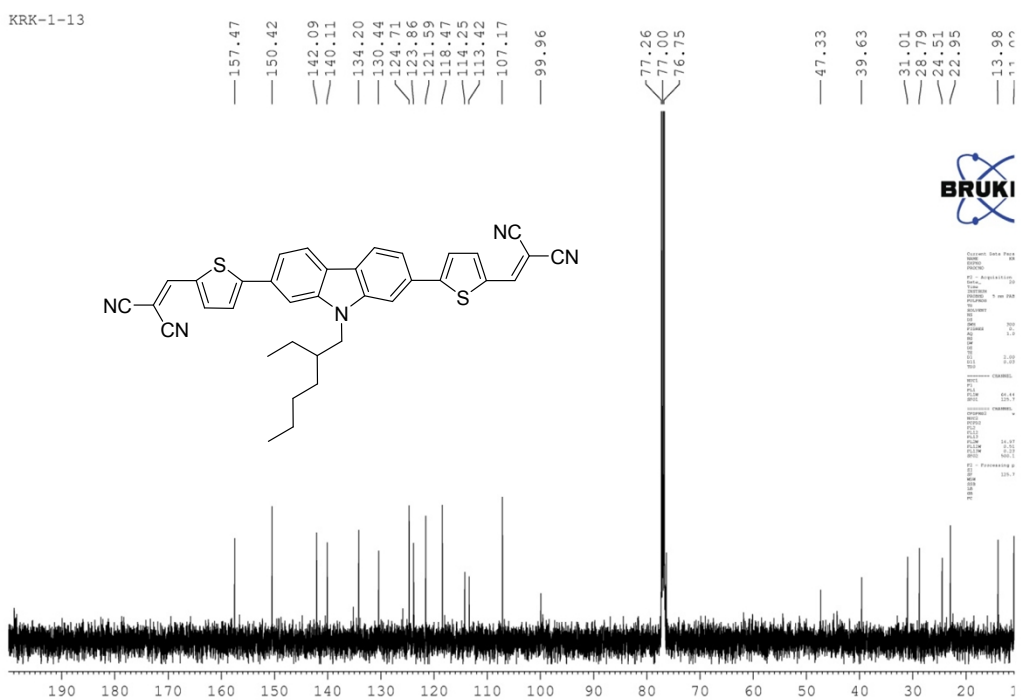


**Fig. S17**  $^{13}\text{C}$  NMR spectra for **3b** in  $\text{CDCl}_3$ .